ISSN 1746-7659, England, UK
Journal of Information and Computing Science
Vol. 14, No. 2, 2019, *pp*.134-148

Bioconvection Peristaltic Transport of Nanofluid in a Channel containing Gyrotactic microorganism

Asha. S. K[1] and Sunitha G[2]
[1]Assistant Professor, Department of Mathematics, Karnatak University, Dharwad-580003, Karnataka, as.kotnur2008@gmail.com
[2] Research Scholars, Department of Mathematics, Karnatak University, Dharwad-580003, Karnataka, India sunithag643@gmail.com
(Received March 03, 2019, accepted April 11, 2019)

Abstract: This research paper is deals with the behavior of gyrotactic in peristaltic transport of nano Eyring-Powell fluid in non-uniform channel. The advantages of adding motile micro-organism to the nanofluid suspension enhanced the heat transfer, mass transfer and improve the nanofluids stability. The governing equations have been fabricated for long wavelength and low Reynolds number assumptions. The solutions have been described for pressure gradient, temperature, nanoparticle concentration and density of motile microorganism equations and solved by using powerful technique known as Homotopy Analysis Method (HAM). Results are reported for different values of the some significant parameters on peristaltic transport through a non-uniform channel and obtained results are displayed in graphs.

Keywords: Biconvection, gyrotactic microorganism, Peristaltic flow, Eyring-Powell fluid model.

1. Introduction

In rheology, the fluids can easily be transport from one region to another region with help of pumping. This type of pumping is known as peristalsis. The peristalsis is a form of fluid flow produced by a continuous wave of area clasping and also compressing propagates of tube or channel. Peristalsis helps in transporting physiological fluids in the human body such as swallowing of food through oesophagus, movement of chime in the gastrointestinal tracts and the vasomotion of small blood vessels. Latham [1] was first initiated the concept of peristaltic mechanism in 1966. After the work of Latham, Jaffrin et al. [2] explore the peristaltic pumping system. They studied the peristaltic flow for the long wavelength and low Reynolds number assumptions. Many researchers and scientist diverted their research interest towards study the peristaltic transport by considering viscous and non-viscous fluids with different models and with different geometries, few references are given in [3-7]. As we know many physiological flows are not uniform. Hence, many of the researchers studied peristaltic flow problems through uniform and non-uniform channels for different fluid models. Some of these investigations have been reported in the references [8-12].

The word “nanofluid” was first formulated by Choi in 1995 [13]. Nanofluid is a liquid that containing nanoparticles with representative length of 1-100nm [14]. The study of nanotechnology based on nanofluids has received general attention due to its applications in engineering and biomedical. Nanofluids are new kind of fluids conceived by destruction of nanometer-sized materials in base fluids such as ethylene-glycol or lubricants, water and silk fibroin etc. Dissimilar nanoparticles have many importances in different fields, like Copper nanoparticles have diverse range of applications in heat transfer systems, sensors and catalysts. In biomedical, magnetite nanoparticles are targeted for magnetic resonance imaging (MRI) and during in drug delivery.In present days, the flow of non-Newtonian fluids has received much awareness due to its applications in medical, industries and technology. To study the non-Newtionian fluids several models have been developed. Among them Eyring-Powell model has certain advantage over other fluid model. Firstly, kinetic theory of liquid is used to obtained the concentrate of fluid model, secondly, at low and high shear rates the concentrate of the model helps to recover the error-free results of viscous nanofluid. Eyring-Powell fluid model was first initiated by Eyring and Powell in 1994 [15]. Many researchers are study the peristaltic flow in different geometrics by considering Eyring-Powell model as cited in references [16-22].

Bioconvection has large amount of applications in biomedical and biotechnology. The bioconvection is defined as flow induced by collective swimming of motile microorganisms which are little denser than water is studied by John [23]. The self- propelled motile microorganisms intensify the base fluid density in a particular direction. Collection of microorganisms at the top of the layer makes suspension more impenetrable than the lower layer due to unstable density distributions. Under such circumference, convection instability and generation of convection patterns take place. Such a quick and random movement pattern of microorganisms causes bioconvection procedure within the system. Bioconvection instability is developed from an initially uniform suspension without an unstable density disturbance was given by Pedley et al. [24]. Many researchers worked on the bioconvection flow with different geometries are given in the ref. [25-27]. In biological fluid mechanics, recent significant growing are nano bioconvection flows. Application of microorganisms is one of the most detectable methods of various bio-methods of nanoparticle production. It is found that the inclusion of particles makes suspension more stable. Kuznetsov et al. [28] studied the suspension of gyrotactic microorganisms in layer of finite depth by adding small solid particles. The nanoparticles are not self-inflicted like motile micro-organisms, nanoparticles motion are due to thermophoresis and Brownian motion. If concentration of nanoparticle is small, bioconvection is occurs in nanofluid. Recent research papers on bioconvection flow containing microorganisms are mentioned in references [29-37].

Literature review revealed that no work has been done on bioconvection peristaltic flow. However, recently Nooren [38] have studied the bioconvection peristaltic flow containing gyrotactic microorganisms in nanofluid in a symmetric channel. Bhatti et al. [39] investigated the peristaltic flow of non- Newtonian Jeffrey nanofluid containing gyrotactic microorganism in annulus. Since, Peristalsis is well known mechanism to transport physiological fluid in most biological organs. Many biological systems are observed to be non-uniform. The purpose of the present study is therefore to understand how the free convection affects the peristaltic transport of blood in a small blood vessel. Here we consider blood as Erying-Powell nanofluid model. The present study has wide range of applications in biomedical science and engineering. Since microorganisms are favorable in decomposition of organic material, producing oxygen and maintaining human health. The dilution of microorganisms in the nanofluids modifies its thermal conductivity. In the present paper, the solution for Pressure gradient, temperature, concentration and motile microorganism's density along with boundary conditions are obtained by using the Homotopy Analysis Method [40, 41]. The effect of various physical parameters on velocity, pressure gradient, temperature and motile-microorganisms density are analysed through graphs.

Mathematical Analysis

Let us consider a peristaltic transport of nano Eyring-Powell fluid in a two dimensional channel. The physical model of the wall surface can be written as

$$\tilde{h}(\tilde{X},\tilde{t}) = a(\tilde{X}) + d\,sin\left(\frac{2\pi}{\lambda}(\tilde{X}-c\tilde{t})\right), \tag{1}$$

here $a(\tilde{X}) = a_{20} + k\tilde{X}$ is the half width of the channel, wavelength of the wall surface is λ, $\tilde{t}$ is the time and d represents the wave amplitude. Let $\tilde{U}$ and $\tilde{V}$ are velocity components along $\tilde{X}$and $\tilde{Y}$directions respectively, the velocity field Vcan be written as

$$V = \left(\tilde{U}(\tilde{X},\tilde{Y},\tilde{t}), \tilde{V}(\tilde{X},\tilde{Y},\tilde{t}), 0\right). \tag{2}$$

The Eyring-Powell fluid model of the shear stress tensor is given by

$$\tilde{S} = \mu\nabla\tilde{V} + \frac{1}{\beta}sinh^{-1}\left(\frac{1}{c^*}\nabla\tilde{V}\right),$$

(3)

where the coefficient of shear viscosity is μ, $\beta$and c^* are the fluid parameters.

$$sinh^{-1}\left(\frac{1}{c^*}\nabla\tilde{V}\right) \approx \frac{1}{c^*} - \frac{1}{6}\left(\frac{1}{c^*}\nabla\tilde{V}\right)^3, \left|\frac{1}{c^*}\nabla\tilde{V}\right| <= 1. \tag{4}$$

The governing equations for the nano Eyring-Powell fluid can be formulated as follows

The continuity equation:

$$\frac{\partial\tilde{U}}{\partial\tilde{X}} + \frac{\partial\tilde{U}}{\partial\tilde{Y}} = 0. \tag{5}$$

The momentum equation:

$$\rho_f\left(\frac{\partial\tilde{U}}{\partial\tilde{t}} + \tilde{U}\frac{\partial\tilde{U}}{\partial\tilde{X}} + \tilde{V}\frac{\partial\tilde{U}}{\partial\tilde{Y}}\right) = -\frac{\partial\tilde{p}}{\partial\tilde{X}} + \left(\mu + \frac{1}{\beta c^*}\right)\left(\frac{\partial^2\tilde{U}}{\partial\tilde{X}^2} + \frac{\partial^2\tilde{U}}{\partial\tilde{Y}^2}\right) - \frac{1}{2\beta c^{*3}}\left(\frac{\partial\tilde{U}}{\partial\tilde{X}} + \frac{\partial\tilde{U}}{\partial\tilde{Y}}\right)^2\left(\frac{\partial^2\tilde{U}}{\partial\tilde{X}^2} + \frac{\partial^2\tilde{U}}{\partial\tilde{Y}^2}\right) + (1 - \phi_1)\rho_f g\beta_1(\tilde{T} - \tilde{T}_0) - (\rho_p - \rho_f)g(\tilde{C} - \tilde{C}_0) - (\rho_m - \rho_f)\gamma g(\tilde{n} - \tilde{n}_0) \tag{6}$$

$$\rho_f\left(\frac{\partial\tilde{V}}{\partial\tilde{t}} + \tilde{U}\frac{\partial\tilde{V}}{\partial\tilde{X}} + \tilde{V}\frac{\partial\tilde{V}}{\partial\tilde{Y}}\right) = -\frac{\partial\tilde{p}}{\partial\tilde{Y}} + \left(\mu + \frac{1}{\beta c^*}\right)\left(\frac{\partial^2\tilde{V}}{\partial\tilde{X}^2} + \frac{\partial^2\tilde{V}}{\partial\tilde{Y}^2}\right) - \frac{1}{2\beta c^{*3}}\left(\frac{\partial\tilde{V}}{\partial\tilde{X}} + \frac{\partial\tilde{V}}{\partial\tilde{Y}}\right)^2\left(\frac{\partial^2\tilde{V}}{\partial\tilde{X}^2} + \frac{\partial^2\tilde{V}}{\partial\tilde{Y}^2}\right). \tag{7}$$

The energy equation

$$(\rho c)_f\left(\frac{\partial \tilde{T}}{\partial \tilde{t}}+\tilde{U}\frac{\partial \tilde{T}}{\partial \tilde{X}}+\tilde{V}\frac{\partial \tilde{T}}{\partial \tilde{Y}}\right)=k^*\left(\frac{\partial^2 \tilde{T}}{\partial \tilde{X}^2}+\frac{\partial^2 \tilde{T}}{\partial \tilde{Y}^2}\right)+(\rho c)_p D_B\left(\frac{\partial \tilde{C}}{\partial \tilde{X}}+\frac{\partial \tilde{C}}{\partial \tilde{Y}}\right)\left(\frac{\partial \tilde{T}}{\partial \tilde{X}}+\frac{\partial \tilde{T}}{\partial \tilde{Y}}\right)+(\rho c)_p\frac{D_T}{T_m}\left(\frac{\partial^2 \tilde{T}}{\partial \tilde{X}^2}+\frac{\partial^2 \tilde{T}}{\partial \tilde{Y}^2}\right)^2. \quad (8)$$

The nanoparticle concentration equation

$$\frac{\partial \tilde{C}}{\partial \tilde{t}}+\tilde{U}\frac{\partial \tilde{C}}{\partial \tilde{X}}+\tilde{V}\frac{\partial \tilde{C}}{\partial \tilde{Y}}=D_B\left(\frac{\partial^2 \tilde{C}}{\partial \tilde{X}^2}+\frac{\partial^2 \tilde{C}}{\partial \tilde{Y}^2}\right)+\frac{D_T}{T_m}\left(\frac{\partial^2 \tilde{T}}{\partial \tilde{X}^2}+\frac{\partial^2 \tilde{T}}{\partial \tilde{Y}^2}\right). \quad (9)$$

The microorganism equation

$$\frac{\partial \tilde{n}}{\partial \tilde{t}}+\tilde{U}\frac{\partial \tilde{n}}{\partial \tilde{X}}+\tilde{V}\frac{\partial \tilde{n}}{\partial \tilde{Y}}=D_n\frac{\partial^2 \tilde{n}}{\partial \tilde{Y}^2}-\frac{bW_C}{(\tilde{C}_1-\tilde{C}_0)}\frac{\partial}{\partial \tilde{Y}}\left(\tilde{n}\frac{\partial \tilde{C}}{\partial \tilde{Y}}\right), \quad (10)$$

where ρ_p is nanoparticle mass density, ρ_f is the density of the fluid, $(\rho c)_f$ and $(\rho c)_p$ are the heat capacity of the fluid and effective heat capacity of the nanoparticle material, thermal conductivity of the fluid is k^*, gravity of acceleration is g, β_1 is volume expansion coefficient, $\tilde{C}$ is the nanoparticle concentration, temperature of the fluid is $\tilde{T}$. Further ρ_f is the effective density, D_B and D_T are the Brownian diffusion and thermophoresis diffusion coefficients, mean fluid temperature is T_m, b and W_C are the chemotaxis and assumed constants, nanoparticles solid volume fraction is ϕ_1. The relationship between the laboratory frame and wave frame are introduced through

$$\tilde{x}=\tilde{X}-c\tilde{t}, \tilde{y}=\tilde{Y},$$
$$\tilde{u}(\tilde{x},\tilde{y})=\tilde{U}-c, \tilde{v}(\tilde{x},\tilde{y})=\tilde{V}, \quad (11)$$

The relevant boundary conditions for the given problem

$$\tilde{\psi}=0, \tilde{u}=\frac{\partial\tilde{\psi}}{\partial\tilde{y}}=0, \tilde{T}=\tilde{T}_0, \tilde{C}=\tilde{C}_0, \tilde{n}=\tilde{n}_0 \text{ at } \tilde{y}=0, \quad (12)$$
$$\tilde{\psi}=q, \tilde{u}=\frac{\partial\tilde{\psi}}{\partial\tilde{y}}=-c, \tilde{T}=\tilde{T}_1, \tilde{C}=\tilde{C}_1, \tilde{n}=\tilde{n}_1 \text{ at } \tilde{y}=\tilde{h}=a(\tilde{x})+d\sin\frac{2\pi}{\lambda}(\tilde{x}).$$

Introducing the following dimensionless variables

$$\left.\begin{aligned}
&\psi=\frac{\tilde{\psi}}{ca}, B=\frac{1}{\mu\beta c^*}, A=\frac{Bc^2}{2a^2c^{*2}}, x=\frac{\tilde{x}}{\lambda}, y=\frac{\tilde{y}}{a}, t=\frac{c\tilde{t}}{\lambda},\\
&v=\frac{\tilde{v}}{c}, \delta=\frac{a}{\lambda}, u=\frac{\tilde{u}}{c}, Re=\frac{\rho_f ca}{\mu}, \beta^*=\frac{k^*}{(\rho c)_f}, Pr=\frac{\nu}{\beta^*}, F=\frac{q}{ca}, p=\frac{a^2\tilde{p}}{c\lambda\mu},\\
&Gr=\frac{(1-\phi_1)\rho_f g\beta_1 a^2(\tilde{T}_1-\tilde{T}_0)}{c\mu}, Nr=\frac{(\rho_p-\rho_f)(\tilde{C}_1-\tilde{C}_0)}{(1-\phi_1)\beta_1(\tilde{T}_1-\tilde{T}_0)\rho_f}, Rb=\frac{(\rho_m-\rho_f)\gamma(\tilde{n}_1-\tilde{n}_0)}{(1-\phi_1)\beta_1(\tilde{T}_1-\tilde{T}_0)\rho_f},\\
&Nb=\frac{(\rho c)_p D_B(\tilde{C}_1-\tilde{C}_0)}{(\rho c)_f\nu}, Nt=\frac{(\rho c)_p D_T(\tilde{T}_1-\tilde{T}_0)}{(\rho c)_f T_m\nu}, \Omega=\frac{\tilde{C}-\tilde{C}_0}{\tilde{C}_1-\tilde{C}_0}, Pe=\frac{bW_C}{D_n}, \sigma=\frac{\tilde{n}_0}{\tilde{n}_1-\tilde{n}_0},\\
&\theta=\frac{\tilde{T}-\tilde{T}_0}{\tilde{T}_1-\tilde{T}_0}, \chi=\frac{\tilde{n}-\tilde{n}_0}{\tilde{n}_1-\tilde{n}_0}, h=\frac{\tilde{h}}{a_{20}}=1+\frac{\lambda kx}{a_{20}}+\alpha\sin 2\pi x, \alpha=\frac{d}{a_{20}}.
\end{aligned}\right\} \quad (13)$$

Where A and B are the dimensionless fluid parameters, Pr is the Prandtl number, Gr is the Grashof number of the local temperature, Nr is the buoyancy ratio respectively, Pe and Rb are the Bioconvection Peclet number and Bioconvection Rayleigh number respectively. Nb is Brownian motion, Nt is thermophoresis parameters and α is the amplitude ratio. The ψ is the stream function given as $u=\frac{\partial\psi}{\partial y}$ and $v=-\delta\frac{\partial\psi}{\partial x}$.

Using the above non-dimensional terms and the basic equations (5)-(10) can be reduce to

$$\frac{\partial p}{\partial x}=(1+B)\frac{\partial^3\psi}{\partial y^3}-A\left(\frac{\partial^2\psi}{\partial y^2}\right)^2\frac{\partial^3\psi}{\partial y^3}+Gr(\theta-Nr\Omega-Rb\chi), \quad (14)$$

$$\frac{\partial p}{\partial y}=0, \quad (15)$$

$$\frac{\partial^2\theta}{\partial y^2}+Pr\,Nb\frac{\partial\theta}{\partial y}\frac{\partial\Omega}{\partial y}+Pr\,Nt\left(\frac{\partial\theta}{\partial y}\right)^2=0, \quad (16)$$

$$\frac{\partial^2\Omega}{\partial y^2}+\frac{Nt}{Nb}\frac{\partial^2\theta}{\partial y^2}=0, \quad (17)$$

$$\frac{\partial^2\chi}{\partial y^2}-Pe\frac{\partial\Omega}{\partial y}\frac{\partial\chi}{\partial y}-Pe\chi\frac{\partial^2\Omega}{\partial y^2}-Pe\sigma\frac{\partial^2\Omega}{\partial y^2}=0. \quad (18)$$

The relevant dimensionless boundary conditions in the wave frame for the problem are defined as

$$\left.\begin{aligned}
&\psi=0, \frac{\partial\psi}{\partial y}=0, \theta=0, \Omega=0, \chi=0 \text{ at } y=0,\\
&\psi=F, \frac{\partial\psi}{\partial y}=-1, \theta=1, \Omega=1, \chi=1 \text{ at } y=h=1+\frac{\lambda kx}{a_{20}}+\alpha\sin 2\pi x,
\end{aligned}\right\} \quad (19)$$

The non-dimensional F is the time mean flow rate in wave frame related to the non-dimensional Θin the laboratory frame as given in the following form

$$F = \int_0^h \frac{\partial \psi}{\partial y} dy, \Theta = F + 1, \tag{20}$$

where $F = \frac{q}{ca}$ and $\Theta = \frac{Q}{ca}$.

2. Solution of the problem

The solutions equations (14)-(18) are obtained by using Homotopy Analysis Method (HAM), the initial guesses and auxiliary linear operators are obtained as

$$\psi_0(y) = \frac{y^2(3Fh - 2Fy + h^4 - hy)}{h^3}, \tag{21}$$

$$\theta_0(y) = \frac{y}{h}, \tag{22}$$

$$\Omega_0(y) = \frac{y}{h}, \tag{23}$$

$$\chi_0(y) = \frac{y}{h}. \tag{24}$$

The relevant auxiliary linear operators are consider as

$$L_\psi = \frac{\partial^3}{\partial y^3}, L_\theta = \frac{\partial^2}{\partial y^2}, L_\Omega = \frac{\partial^2}{\partial y^2}, L_\chi = \frac{\partial^2}{\partial y^2}, \tag{25}$$

which satisfies the properties

$$L_\psi\left[C_1 + C_2 y + C_3 \frac{y^2}{2}\right] = 0, L_\theta[C_4 + C_5 y] = 0, L_\Omega[C_6 + C_7 y] = 0, L_\chi[C_8 + C_9 y] = 0, \tag{26}$$

The solutions are easily found coupled equations together with boundary conditions. Using the methodology of the given method, solutions are written as follows

$$\psi(y,q) = \left(\frac{3F}{h^2} - \frac{1}{h}\right)y^2 - \left(\frac{2F}{h^3} + \frac{1}{h^2}\right)y^3 + h_\psi{}^2 a_{11} + h_\psi{}^3 a_{12} + h_\psi{}^4 a_{13} + h_\psi{}^5 a_{14}$$
$$+ h_\psi{}^5\left[\left(\left(\frac{h_\theta}{24h} - Nr\frac{h_\Omega}{24h}\left(1 + \frac{Nt}{Nb}\right) - Rb\frac{h_\chi}{24h}(1 - Pe\sigma)\right)\right)y^4 + \left(\frac{Pr\,Nb}{120h^2} + \frac{Pr\,Nt}{120h^2} + \frac{Pr\,Pe}{120h^2}\right)y^5\right], \tag{27}$$

$$\theta(y,q) = \frac{y}{h} + h_\theta{}^2\left(\frac{y}{h} + \Pr Nb\left(1 + \frac{Nt}{Nb}\right)\frac{y^2}{2h^2}\right) + h_\theta{}^3\frac{y}{h} + h_\theta{}^3 \Pr Nb\left(1 + \frac{Nt}{Nb}\right)\frac{y^2}{2h^2}$$
$$+ h_\theta{}^4 \Pr^2\left(1 + \frac{Nt}{Nb}\right)\left(h_\Omega\frac{Nt}{Nb} + h_\Omega Nt + 2\right)\frac{y^3}{6h^3} + h_\theta{}^4 \Pr^2 NtNb\left(1 + \frac{Nt}{Nb}\right)\frac{y^3}{6h^3}. \tag{28}$$

$$\Omega(y,q) = \frac{y}{h} + h_\Omega{}^2\left(1 + \frac{Nt}{Nb}\right)\frac{y}{h} + h_\Omega{}^3\left(1 + \frac{Nt}{Nb}\right)\frac{y}{h} + h_\Omega{}^4\left(1 + \frac{Nt}{Nb}\right)\frac{y}{h}$$
$$+ h_\Omega{}^3 h_\theta\frac{Nt}{Nb}\frac{y}{h} + h_\Omega{}^3 h_\theta\, Pr\, N\, t\left(1 + \frac{Nt}{Nb}\right)\frac{y^2}{2h^2}. \tag{29}$$

$$\chi(y,q) = \frac{y}{h} + h_\chi{}^2\left(\frac{y}{h} - Pe\frac{y^2}{2h^2} - Pe\sigma\frac{y}{h}\right) + h_\theta{}^3\left((1 - Pe\sigma)\frac{y}{h} - Pe\frac{y^2}{2h^2}\right) +$$
$$h_\chi{}^4\left((1 - Pe\sigma)\frac{y}{h} - \left(1 + h_\Omega - h_\Omega Pe\sigma + h_\Omega\frac{Nt}{Nb} - h_\Omega Pe\sigma\frac{Nt}{Nb}\right)Pe\frac{y^2}{2h^2}\right) - h_\Omega Pe^2\left(1 + \frac{Nt}{Nb}\right)\frac{y^3}{6h^3}. \tag{30}$$

$$u(y,q) = 2\left(\frac{3F}{h^2} - \frac{1}{h}\right)y - 3\left(\frac{2F}{h^3} + \frac{1}{h^2}\right)y^2 + h_\psi{}^2 b_{11} + h_\psi{}^3 b_{12} + h_\psi{}^4 b_{13} + h_\psi{}^5 b_{14}$$
$$+ h_\psi{}^5\left[\left(\left(\frac{h_\theta}{24h} - Nr\frac{h_\Omega}{24h}\left(1 + \frac{Nt}{Nb}\right) - Rb\frac{h_\chi}{24h}(1 - Pe\sigma)\right)\right)4y^3 + \left(\frac{Pr\,Nb}{120h^2} + \frac{Pr\,Nt}{120h^2} + \frac{Pr\,Pe}{120h^2}\right)5y^4\right], \tag{31}$$

The wave frame of volumetric flow rate is defined as

$$Q(x,t) = \int_0^h u(y,q)dy. \tag{32}$$

The pressure gradient expression can be written in the form as below

$$\frac{\partial p}{\partial x} = \left(\frac{Q - \left(\frac{1}{3} + \frac{4F}{3h}\right)h^2 + \left(\frac{2F}{h^3} + \frac{1}{h^2}\right)h^3 - h_\psi{}^2 c_{11} - h_\psi{}^3 c_{12} - h_\psi{}^4 c_{13} - h_\psi{}^5 c_{14} - h_\psi{}^5 c_{15}}{-h_\psi{}^2\frac{h^3}{6} - 2h_\psi{}^3\frac{h^3}{6} + h_\psi{}^4(1+B)\frac{h^3}{6} + h_\psi{}^5 c_{14} + h_\psi{}^5 c_{15}}\right). \tag{33}$$

Graphical Analysis

This section represents the detailed analysis of the various physical parameters of pressure gradient, temperature, nanoparticle concentration and motile microorganism density profile.

Pressure gradient profile

In Figures (1) describe the flow behavior of various physical parameters on pressure gradient profile. Figure 1(a) and figure 1(b) are described to show the flow behavior of fluid parameters A and B. It is observed that fluid parameter have opposite behavior on pressure gradient. Fluid parameter A increases with an increasing pressure gradient, which occurs the non-linear part of the momentum equation, in the considerable part of the channel is comparatively dwarf$x \in [0,0.2]$and$x \in [0.5,0.6]$ the pressure gradient is relatively small and the flow can easily pass without forcing of large pressure gradient. However, the tapered part of channel is $x \in [0.3,0.5]$ as much immense pressure gradient is required to maintain the same flux to pass through it. Besides, we have observed that fluid parameter B increases on pressure gradient (>0) increased. Since$B = \frac{1}{\mu\beta c}$, by increasing B the viscosity of fluid μ decreases, which cause decreases in pressure. Figures 1(c) and 1(d) are plotted to show the effect of Grashof number and buoyancy ratio pressure gradient. Through this figures one can be observed that pressure decreases for both the parameters. In figure 1(e) depicted Biconvection Rayleigh parameter effect on pressure. When Biconvection Rayleigh parameter increases the pressure gradient is decreased. This is due convection instability take place and that cause convection pattern which decrease the pressure gradient.

Temperature profile

Figure 2 is plotted to show the behavior of physical parametersNb,NtandPron the temperature distribution θ by fixing other physical parameters. Figure 2(a) reveals that the temperature profile is decreasing, when the Brownian motion parameterNb is increased. Thermophoresis parameter variationon on temperature profile is showed in figure 2(b). We observed that the temperature appears to be increases when thermophoresis parameter Nt is increased, since the collision between the particles enhances which produce plenty of heat, as a results in raises of temperature. The Figure 2(c) describes the Prandtl number effect. Observe that Prandtl number increases on temperature profile increased.

Concentration profile

In figure (3) shows about the various physical parameters Nt , Nb and Pr on nanoparticles concentration profile Ω. In figure 3(a), we have to observe that motion of nanoparticles increases with increase of Brownian motion parameter. The fact is due to transfer of nanoparticle from cold region to hot region which yield the increment of concentration distribution. Figure 3(b) shows the consequence of thermophoresis parameter. When the thermophoresis parameter increases the concentration decreases. The decrease in nanoparticles concentration is due to interference in fluid molecules. Since, in thermophoresis, where the particles are moved away from the hot region to cold region, which results the disturbance in nanoparticle and hence there is decrease in concentration of nanoparticles. The figure 3(c) describes the flow of nanoparticle concentration decreases when the Prandtl number is increased. As the Prandtl number Princreases the thermal conductivity of the fluid decreases thus the concentration of nanoparticle decreases.

Density of Motile microorganism profile

Figure 4 is plotted for the various flow behavior of the motile microorganism profile for different physical parameters. From figure 4(a), one can observed that the density of motile microorganism profile increases with an increase of Brownian motion parameterNb. It is obvious that motile microorganism transfer rate increases when$Nb$is increased. Figure 4(b) depicted the thermophoresis parameter effect on the motile microorganism density, it is noticed that density of motile microorganism profile decreased when the thermophoresis parameter Nt increases. Enhancement in Nt brings the nanoparticle at higher state heat region which enhance the fluid temperature. Hence the density of microorganism decreases. Figure 4(c) express the Biconvection Peclet number decreases with decrease of motile microorganism density. In Figure 4(d) shows the effect Biconvection constant σ on motile microorganism density. The motile microorganism density appears to be decreases when Biconvection constant is increased.

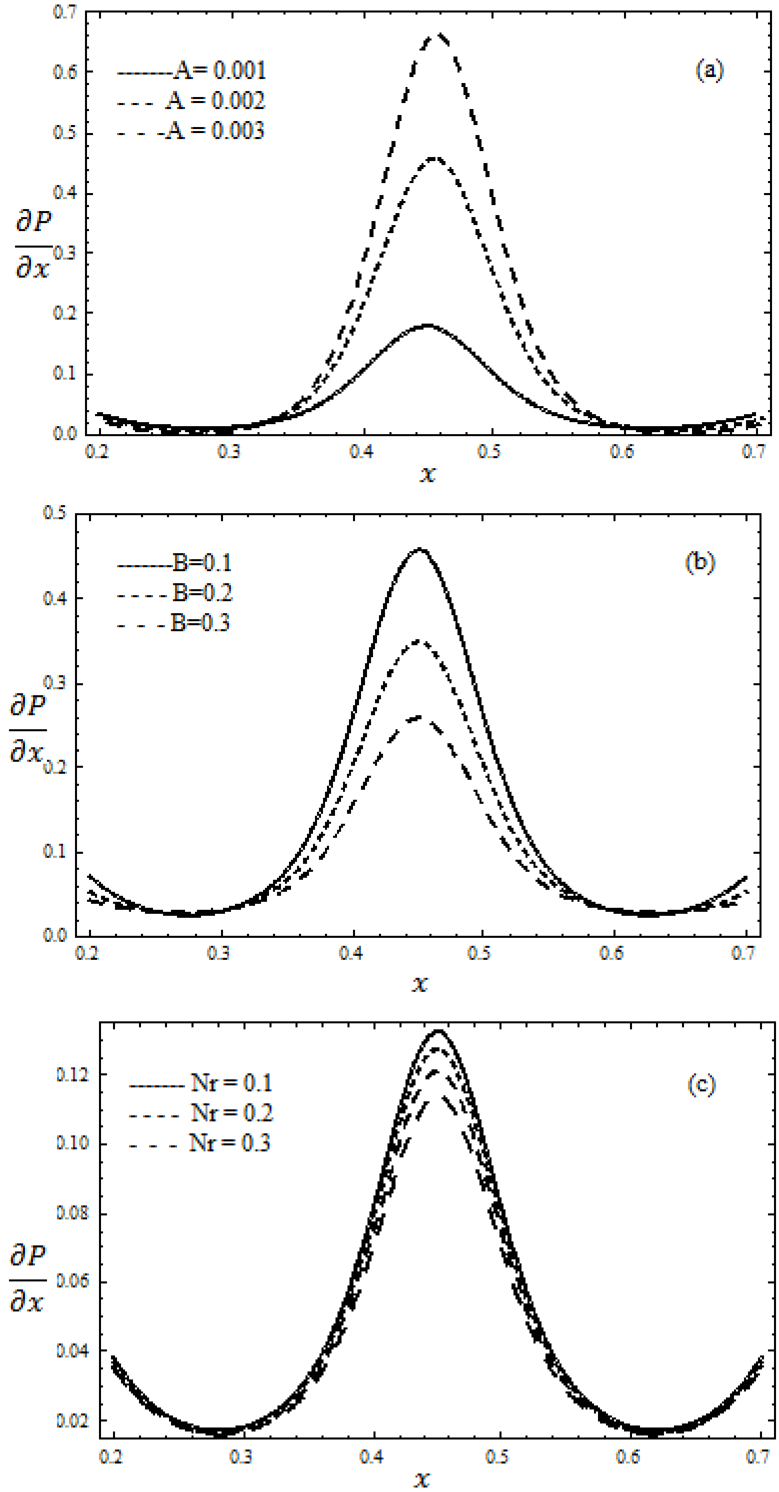
-------A= 0.001
- - - A = 0.002
- - -A = 0.003
(a)
$\frac{\partial P}{\partial x}$
x
-------B=0.1
- - - - B=0.2
- - - B=0.3
(b)
$\frac{\partial P}{\partial x}$
x
------- Nr = 0.1
- - - - Nr = 0.2
- - - Nr = 0.3
(c)
$\frac{\partial P}{\partial x}$
x

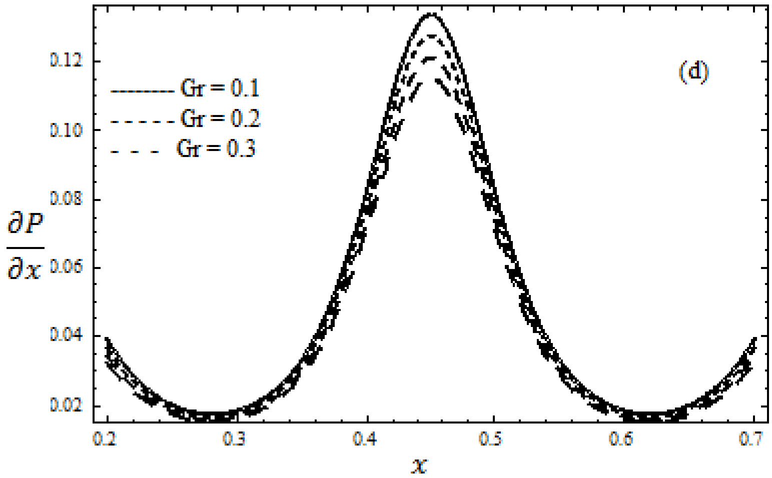

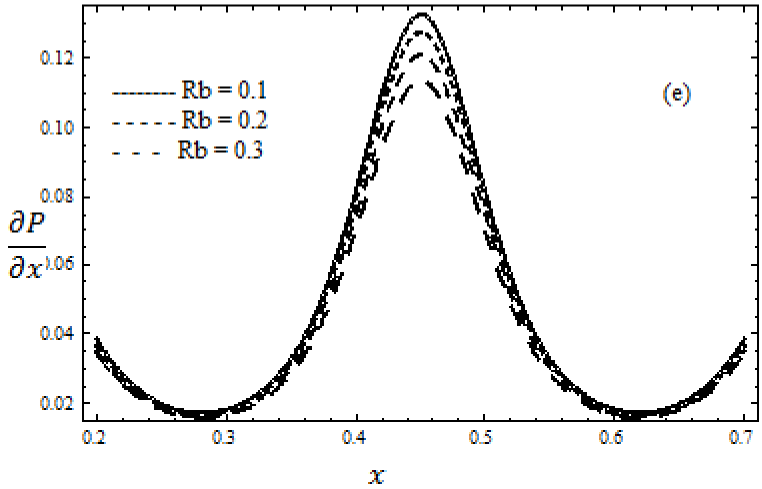

Fig. 1 $\frac{dp}{dx}$ to x, when $t = 0.1$, $x = 0.2$, Pr = 6.9, $\varphi = 0.6$,Q=0.25, λ =10, k =0.1, a_{20}=2.0,σ =0.5, Nt=0.4, Nb=0.4; (a) Gr=1.5, Nr=1.5, Rb=1.5, B=2.0. (b)A=0.001, Gr=1.5, Nr=1.5, Rb=1.5. (c) A=0.001, B=2.0, Nr=1.5, Rb=1.5. (d)A=0.001, B=2.0, Gr=1.5, Rb=1.5. (e)A=0.001, B=2.0, Gr=0.4, Nr=0.3.

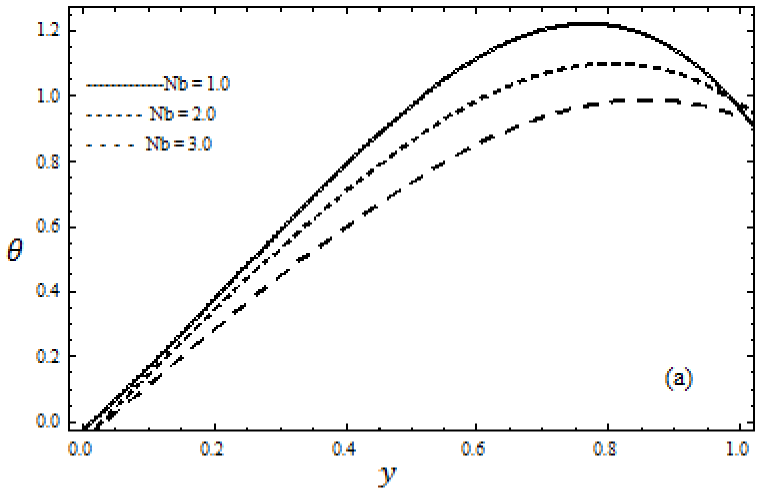

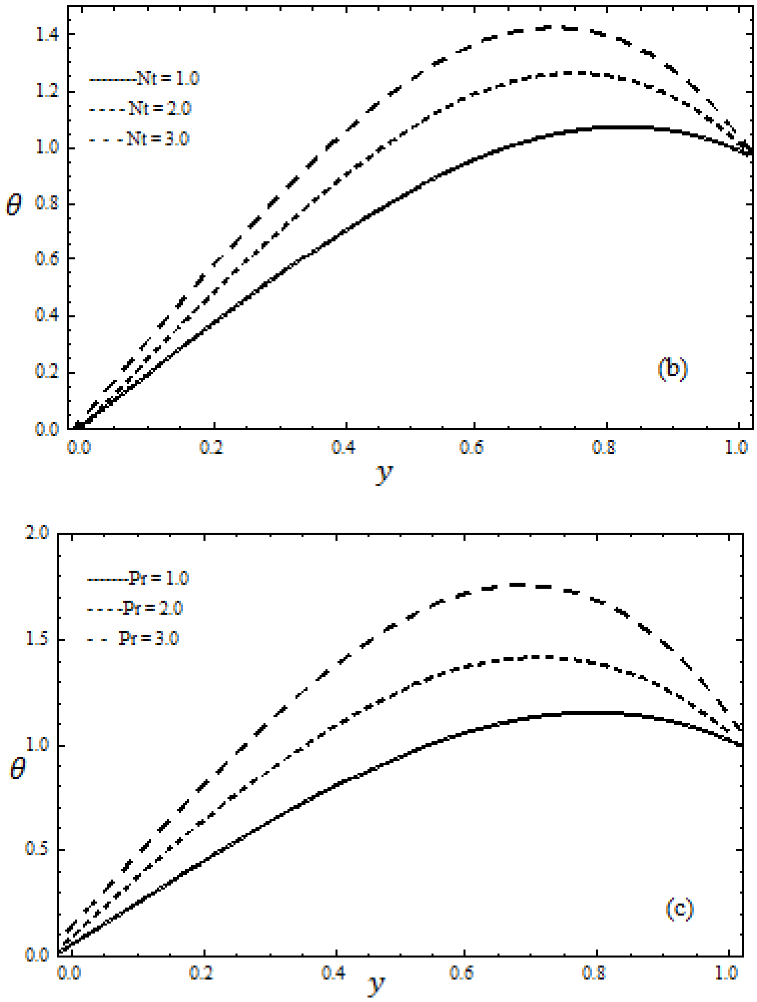

Fig. 2 Temperature θ versus y when $t = 0.1$, $x = 0.2$, $\varphi = 0.6$, Q=0.25, λ =10, k =0.1, a_{20}=2.0; (a)Nt=0.4, Pr=6.9. (b)Pr=6.9, Nb=0.4. (c) Nt=0.4, Nb=0.4.

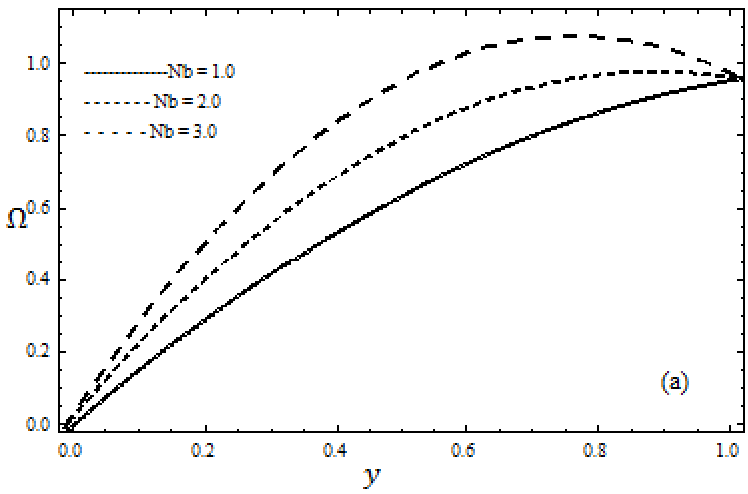

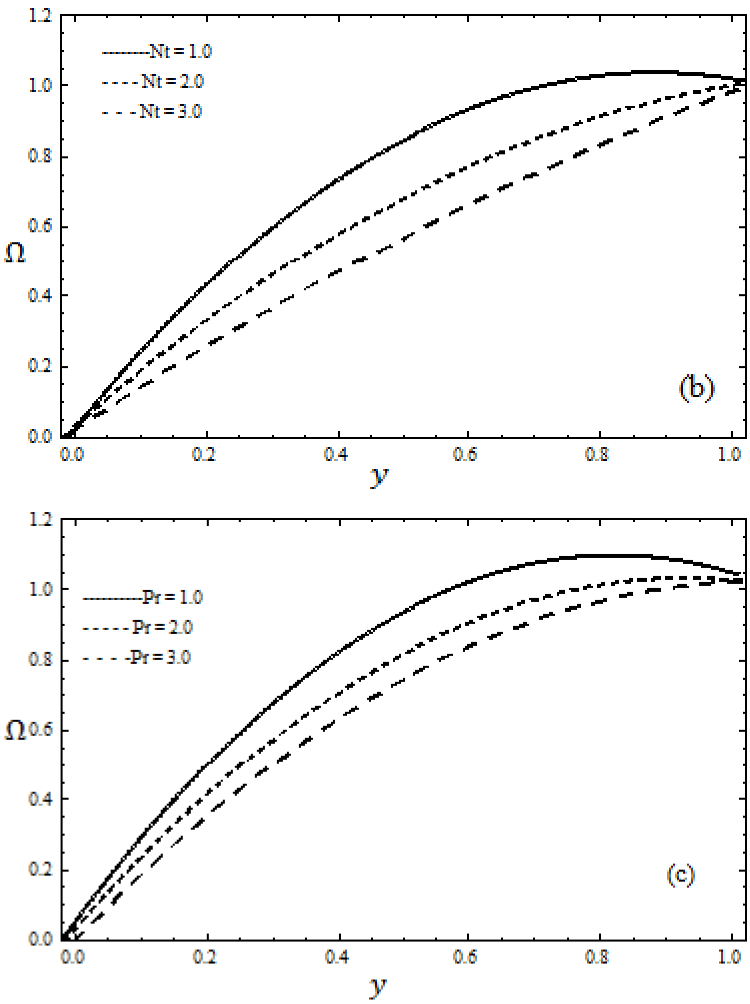

Fig. 3 Concentration Ω versus y when $t = 0.1$, $x = 0.2$, $\varphi = 0.6$, Q=0.25, λ =10, k =0.1, a_{20}=2.0; (a) Nt=0.4, Pr=6.9. (b) Pr=6.9, Nb=0.4. (c) Nt=0.4, Nb=0.4.

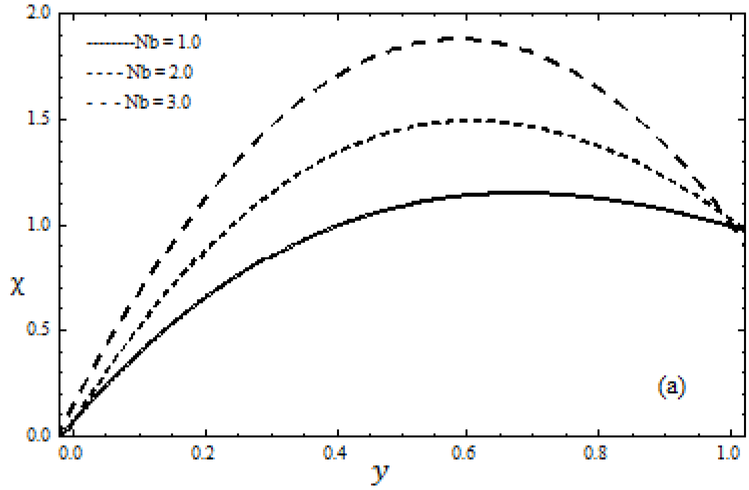

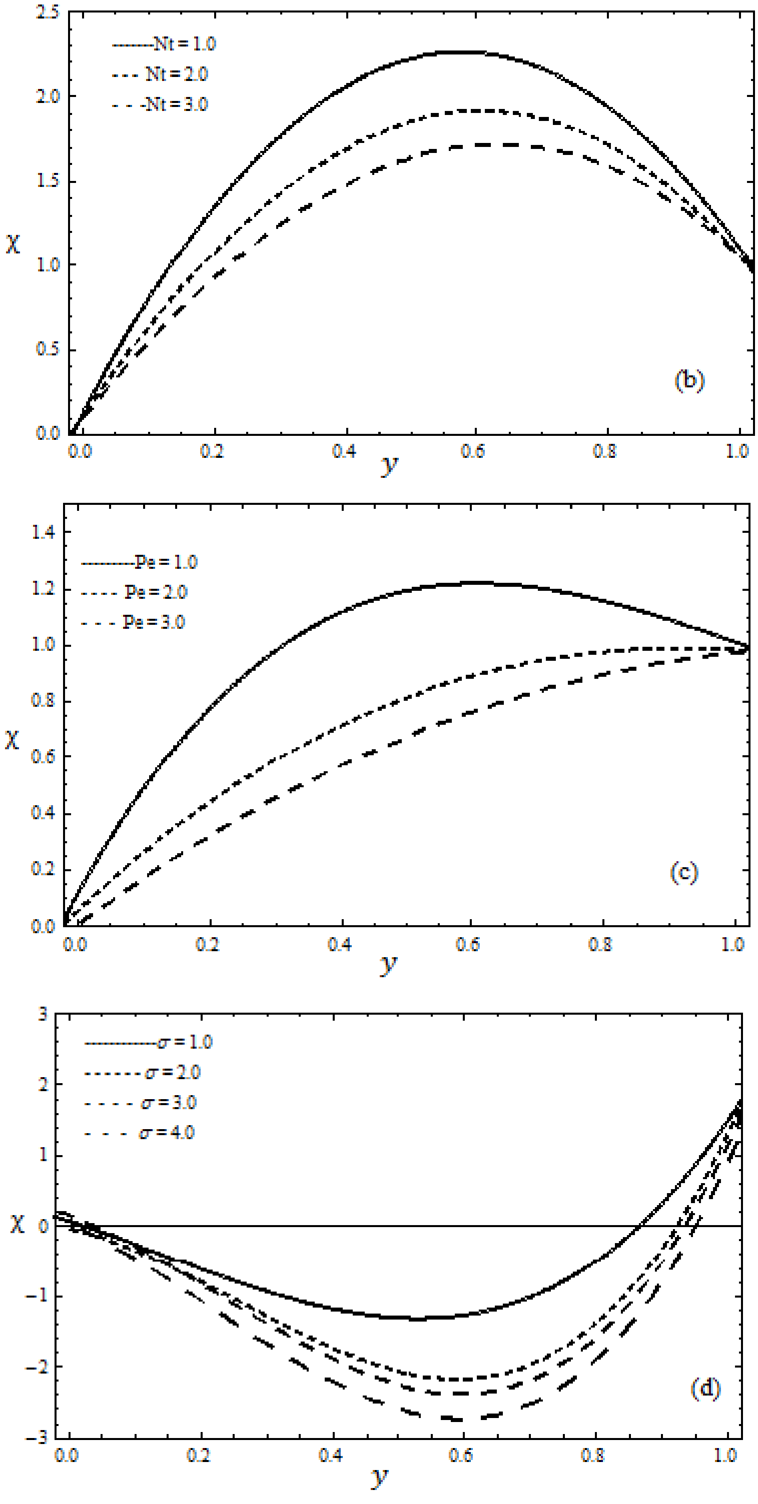

Fig. 4 Motile microorganism densityversus ywhen $t = 0.1$, $x = 0.2$, Pr = 6.9, $\varphi = 0.6$, Q=0.25, λ =10, k =0.1, a_{20}=2.0; (a)σ =0.5, Nt=0.4, Pe=2.0. (b) σ =0.5, Nb=0.4, Pe=2.0. (c)Nb=0.4, σ =0.5, Nt=0.4.(d)Pe=2.0, Nt=0.4, Nb=0.4.

Concluding remarks

Here we analyzed the Biconvection peristaltic flow of a nano Eyring-Powell fluid through non-uniform channel containing gyrotactic microorganism is investigated under long wavelength and low Reynolds number approximations. The results are displayed in the form of graphs and following the important points are mentioned below.

- Pressure gradient gives opposite behavior with an increasing values of Eyring-Powell fluid parameters *A* and *B*.

- Opposite behavior of nanoparticle concentration and temperature profiles increases with an Brownian motion parameter (Nb), thermophoresis parameter (Nt), Prandtl number (Pr).
- Pressure gradient profile decreases with an increasing values of Grashof number(Gr), buoyancy ratio (Nr) and Bioconvection Rayleigh number(Rb).
- Densityof Motile microorganism gives the opposite outcomes an increasing values of Brownian motion parameter(Nb), thermophoresis parameter(Nt).
- Similar behavior for density of motile microorganism profile increases with an increasing values of Bioconvection Peclet number(Pe), Bioconvection constant (σ).

Acknowledgement

Author Asha S. K acknowledge the kind support of the UGC (F510/3/DRS-III/2016(SAP-I)) dated:29/02/2016. The author Sunitha G acknowledge to UGC for financial support under NFST scheme (201718-NFST-KAR-01215) dated: 01/04/2017.

Appendix: supplementary data.

The values of a11, a12, a13, a14 in Eq. (35) are written in the below:

$$a_{11} = -\frac{\partial p}{\partial x}\frac{y^3}{6} + (1+B)\left[\left(\frac{3F}{h^2}-\frac{1}{h}\right)y^2 - \left(\frac{2F}{h^3}-\frac{1}{h^2}\right)y^3\right] + Gr\left(\frac{y^4}{24h} - Nr\frac{y^4}{24h} - Rb\frac{y^4}{24h}\right)$$
$$-\frac{A(12F-6h)}{h^9}\left(\left(6Fh+2h^2\right)^2\frac{y^3}{6} + (12F+6h)^2\frac{y^5}{60} - 2\left(6Fh+2h^2\right)(12F+6h)\frac{y^4}{24}\right)$$

$$a_{12} = -2\frac{\partial p}{\partial x}\frac{y^3}{6} + (1+B)\left[\left(\frac{3F}{h^2}-\frac{1}{h}\right)y^2 - \left(\frac{2F}{h^3}-\frac{1}{h^2}\right)y^3\right] + Gr\left(\frac{y^4}{24h} - Nr\frac{y^4}{24h} - Rb\frac{y^4}{24h}\right)$$
$$-\frac{A(12F-6h)}{h^9}\left(\left(6Fh+2h^2\right)^2\frac{y^3}{6} + (12F+6h)^2\frac{y^5}{60} - 2\left(6Fh+2h^2\right)(12F+6h)\frac{y^4}{24}\right)$$

$$a_{13} = (1+B)\frac{\partial p}{\partial x}\frac{y^3}{6} + (1+B)^2\left[\left(\frac{3F}{h^2}-\frac{1}{h}\right)y^2 - \left(\frac{2F}{h^3}-\frac{1}{h^2}\right)y^3\right] + (1+B)Gr\left(\frac{y^4}{24h} - Nr\frac{y^4}{24h} - Rb\frac{y^4}{24h}\right)$$
$$-\frac{A(1+B)(12F-6h)}{h^9}\left(\left(6Fh+2h^2\right)^2\frac{y^3}{6} + (12F+6h)^2\frac{y^5}{60} - 2\left(6Fh+2h^2\right)(12F+6h)\frac{y^4}{24}\right)$$

$$a_{14} = \left(\frac{\partial p}{\partial x} + 6(1+B)\left(\frac{2F}{h^3}-\frac{1}{h^2}\right) + \frac{A(12F-6h)}{h^9}\left(6Fh+2h^2\right)^2\right)$$
$$\left(\begin{array}{l} 4(1+B)^2\left(\frac{3F}{h^2}-\frac{1}{h}\right)^2\frac{y^{12}}{12!} + \frac{A(12F-6h)}{h^9}\left(6Fh+2h^2\right)^2\frac{y^4}{24} - 4(1+B)\left(\frac{3F}{h^2}-\frac{1}{h}\right) \\ \left(\frac{\partial p}{\partial x} + 6(1+B)\left(\frac{2F}{h^3}-\frac{1}{h^2}\right)\right)\frac{y^4}{24} - \left(\left(\frac{\partial p}{\partial x} + 6(1+B)\left(\frac{2F}{h^3}-\frac{1}{h^2}\right) + \frac{A(12F-6h)}{h^9}\left(6Fh+2h^2\right)^2\right)^2\right)\frac{y^5}{60} \\ -4(1+B)\left(\frac{3F}{h^2}-\frac{1}{h}\right)\left[\frac{A(12F-6h)}{h^9}\left(6Fh+2h^2\right)^2(12F-6h) + Gr\left(\frac{1}{2h}-\frac{Nr}{2h}-\frac{Rb}{2h}\right)\right]\frac{y^5}{60} \end{array}\right)$$
$$-\left(\begin{array}{l} 4(1+B)\left(\frac{3F}{h^2}-\frac{1}{h}\right)\frac{A(12F-6h)}{3h^9}(12F+6h)^2 + 2\left(\begin{array}{l}\frac{\partial p}{\partial x} + 6(1+B)\left(\frac{2F}{h^3}+\frac{1}{h^2}\right) \\ +\frac{A(12F-6h)}{h^9}\left(6Fh+2h^2\right)^2\end{array}\right) \\ \left[\frac{A(12F-6h)}{3h^9}(12F+6h)^2\right] \end{array}\right)\frac{y^6}{5!}$$
$$+\left(\begin{array}{l} \frac{A(12F-6h)}{h^9}\left(6Fh+2h^2\right)(12F+6h) + 2\left(\begin{array}{l}\frac{\partial p}{\partial x} + 6(1+B)\left(\frac{2F}{h^3}+\frac{1}{h^2}\right) \\ +\frac{A(12F-6h)}{h^9}\left(6Fh+2h^2\right)^2\end{array}\right) \\ \left[\frac{A(12F-6h)}{3h^9}(12F+6h)^2\right] \end{array}\right)\frac{y^7}{210}$$

$$-2\left(\frac{A(12F-6h)}{h^9}(6Fh+2h^2)(12F+6h)+Gr\left(\frac{1}{2h}-\frac{Nr}{2h}-\frac{Rb}{2h}\right)\right)\left[\frac{A(12F-6h)}{3h^9}(12F+6h)^2\right]\frac{y^8}{336}$$

The values of b11, b12, b13, b14 in Eq. (39) are written in the below:

$$b_{11}=-\frac{\partial p}{\partial x}\frac{y^2}{2}+(1+B)\left[2\left(\frac{3F}{h^2}-\frac{1}{h}\right)y-3\left(\frac{2F}{h^3}+\frac{1}{h^2}\right)y^2\right]+Gr\left(\frac{y^3}{6h}-Nr\frac{y^3}{6h}-Rb\frac{y^3}{6h}\right)$$
$$-\frac{A(12F-6h)}{h^9}\left(\left(6Fh+2h^2\right)^2\frac{y^2}{2}+(12F+6h)^2\frac{y^4}{12}-2\left(6Fh+2h^2\right)(12F+6h)\frac{y^3}{6}\right)$$

$$b_{12}=-\frac{\partial p}{\partial x}y^2+(1+B)\left[2\left(\frac{3F}{h^2}-\frac{1}{h}\right)y-3\left(\frac{2F}{h^3}+\frac{1}{h^2}\right)y^2\right]+Gr\left(\frac{y^3}{6h}-Nr\frac{y^3}{6h}-Rb\frac{y^3}{6h}\right)$$
$$-\frac{A(12F-6h)}{h^9}\left(\left(6Fh+2h^2\right)^2\frac{y^2}{2}+(12F+6h)^2\frac{y^4}{12}-2\left(6Fh+2h^2\right)(12F+6h)\frac{y^3}{6}\right)$$

$$b_{13}=(1+B)\frac{\partial p}{\partial x}\frac{y^2}{2}+2(1+B)^2\left(\frac{3F}{h^2}-\frac{1}{h}\right)y-3(1+B)^2\left(\frac{2F}{h^3}+\frac{1}{h^2}\right)y^2+(1$$
$$+B)Gr\left(\frac{y^3}{6h}-Nr\frac{y^3}{6h}-Rb\frac{y^3}{6h}\right)$$
$$-\frac{A(1+B)(12F-6h)}{h^9}\left(\left(6Fh+2h^2\right)^2\frac{y^2}{2}+(12F+6h)^2\frac{y^3}{6}-2\left(6Fh+2h^2\right)(12F+6h)\frac{y^3}{6}\right)$$

$$b_{14}=\left(\frac{\partial p}{\partial x}+6(1+B)\left(\frac{2F}{h^3}-\frac{1}{h^2}\right)+\frac{A(12F-6h)}{h^9}\left(6Fh+2h^2\right)^2\right)$$

$$\left(\begin{array}{l}4(1+B)^2\left(\frac{3F}{h^2}-\frac{1}{h}\right)^2\frac{y^2}{2!}-4(1+B)\left(\frac{3F}{h^2}-\frac{1}{h}\right)\left(\begin{array}{l}\frac{\partial p}{\partial x}+6(1+B)\left(\frac{2F}{h^3}+\frac{1}{h^2}\right)+\\\left(\frac{A(12F-6h)}{h^9}\left(6Fh+2h^2\right)^2\right)^2\end{array}\right)\frac{y^3}{6}\\-\left(\frac{\partial p}{\partial x}+6(1+B)\left(\frac{2F}{h^3}+\frac{1}{h^2}\right)+\left(\frac{A(12F-6h)}{h^9}\left(6Fh+2h^2\right)^2\right)^2\right)^2-4(1+B)\left(\frac{3F}{h^2}-\frac{1}{h}\right)\\\left[\frac{A(12F-6h)}{h^9}\left(6Fh+2h^2\right)^2(12F-6h)+Gr\left(\frac{1}{2h}-\frac{Nr}{2h}-\frac{Rb}{2h}\right)\right]\frac{y^4}{12}\end{array}\right)$$

$$-\left(\begin{array}{l}4(1+B)\left(\frac{3F}{h^2}-\frac{1}{h}\right)\frac{A(12F-6h)}{3h^9}(12F+6h)^2+2\left(\begin{array}{l}\frac{\partial p}{\partial x}+6(1+B)\left(\frac{2F}{h^3}+\frac{1}{h^2}\right)+\\\frac{A(12F-6h)}{h^9}\left(6Fh+2h^2\right)^2\end{array}\right)\\\left[A(12F-6h)(12F+6h)^2\right](12F+6h)+Gr\left(\frac{1}{2h}-\frac{Nr}{2h}-\frac{Rb}{2h}\right)\end{array}\right)\frac{y^5}{20}$$

$$+\left(\begin{array}{l}\frac{A(12F-6h)}{h^9}\left(6Fh+2h^2\right)(12F+6h)+2\left(\begin{array}{l}6(1+B)\left(\frac{2F}{h^3}+\frac{1}{h^2}\right)\\+\frac{A(12F-6h)}{h^9}\left(6Fh+2h^2\right)^2\end{array}\right)\\\left[\frac{A(12F-6h)}{3h^9}(12F+6h)^2\right]\end{array}\right)\frac{y^6}{30}$$

$$-2\left(\frac{A(12F-6h)}{h^9}(6Fh+2h^2)(12F+6h)+Gr\left(\frac{1}{2h}-\frac{Nr}{2h}-\frac{Rb}{2h}\right)\right)\left[\frac{A(12F-6h)}{2h^9}(12F+6h)^2\right]\frac{y^7}{41}$$

The values of c11, c12, c13, c14, c15 in Eq. (41) are written in the below:

$$c_{11}=(1+B)\left[\left(\frac{3F}{h^2}-\frac{1}{h}\right)h^2-\left(\frac{2F}{h^3}+\frac{1}{h^2}\right)h^3\right]+Gr\left(\frac{h^3}{24}-Nr\frac{h^3}{24}-Rb\frac{h^3}{24}\right)$$

$$-\frac{A(12F-6h)}{h^9}\left(\left(6Fh+2h^2\right)^2\frac{h^3}{6}+(12F+6h)^2\frac{h^5}{60}-2\left(6Fh+2h^2\right)(12F+6h)\frac{h^4}{24}\right)c_{12}$$

$$=(1+B)\left(\frac{3F}{h^2}-\frac{1}{h}\right)h^2-\left(\frac{2F}{h^3}+\frac{1}{h^2}\right)h^3+Gr\left(\frac{h^3}{24}-Nr\frac{h^3}{24}-Rb\frac{h^3}{24}\right)$$

$$-\frac{A(12F-6h)}{h^9}\left(\left(6Fh+2h^2\right)^2\frac{h^3}{6}+(12F+6h)^2\frac{h^5}{60}-2\left(6Fh+2h^2\right)(12F+6h)\frac{h^4}{24}\right)$$

$$c_{14}=\left(6(1+B)\left(\frac{2F}{h^3}+\frac{1}{h^2}\right)+\frac{A(12F-6h)}{h^9}\left(6Fh+2h^2\right)^2\right)$$

$$\left(\begin{array}{l}4(1+B)^2\left(\frac{3F}{h^2}-\frac{1}{h}\right)^2\frac{h^3}{3!}-4(1+B)\left(\frac{3F}{h^2}-\frac{1}{h}\right)\left(\begin{array}{l}6(1+B)\left(\frac{2F}{h^3}+\frac{1}{h^2}\right)+\\ \frac{A(12F-6h)}{h^9}\left(6Fh+2h^2\right)^2\end{array}\right)\frac{h^4}{4!}\\ -\left(6(1+B)\left(\frac{2F}{h^3}+\frac{1}{h^2}\right)+\left(\frac{A(12F-6h)}{h^9}\left(6Fh+2h^2\right)^2\right)^2\right)^2-4(1+B)\left(\frac{3F}{h^2}-\frac{1}{h}\right)\\ \left[\frac{A(12F-6h)}{h^9}\left(6Fh+2h^2\right)^2(12F-6h)+Gr\left(\frac{1}{2h}-\frac{Nr}{2h}-\frac{Rb}{2h}\right)\right]\end{array}\right)\frac{h^5}{60}$$

$$-\left(\begin{array}{l}4(1+B)\left(\frac{3F}{h^2}-\frac{1}{h}\right)\frac{A(12F-6h)}{3h^9}(12F+6h)^2+2\left(\begin{array}{l}6(1+B)\left(\frac{2F}{h^3}+\frac{1}{h^2}\right)+\\ \frac{A(12F-6h)}{h^9}\left(6Fh+2h^2\right)^2\end{array}\right)\\ \left[A(12F-6h)(12F+6h)^2\right](12F+6h)+Gr\left(\frac{1}{2h}-\frac{Nr}{2h}-\frac{Rb}{2h}\right)\end{array}\right)\frac{h^6}{120}$$

$$+\left(\begin{array}{l}\left(\frac{A(12F-6h)}{h^9}\left(6Fh+2h^2\right)(12F+6h)+Gr\left(\frac{1}{2h}-\frac{Nr}{2h}-\frac{Rb}{2h}\right)\right)^2+2\left(\begin{array}{l}6+6(1+B)\left(\frac{2F}{h^3}+\frac{1}{h^2}\right)+\\ \frac{A(12F-6h)}{h^9}\left(6Fh+2h^2\right)^2\end{array}\right)\\ \left[\frac{A(12F-6h)}{3h^9}(12F+6h)^2\right]\end{array}\right)\frac{h^7}{210}$$

$$-2\left(\frac{A(12F-6h)}{h^9}\left(6Fh+2h^2\right)(12F+6h)+Gr\left(\frac{1}{2h}-\frac{Nr}{2h}-\frac{Rb}{2h}\right)\right)\left[\frac{A(12F-6h)}{2h^9}(12F+6h)^2\right]\frac{h^8}{336}c_{13}$$

$$=(1+B)^2\left(\frac{3F}{h^2}-\frac{1}{h}\right)h^2-(1+B)^2\left(\frac{2F}{h^3}+\frac{1}{h^2}\right)h^3+(1+B)Gr\left(\frac{h^3}{24}-Nr\frac{h^3}{24}-Rb\frac{h^3}{24}\right)$$

$$-\frac{A(1+B)(12F-6h)}{h^9}\left(\left(6Fh+2h^2\right)^2\frac{h^3}{6}+(12F+6h)^2h^5-2\left(6Fh+2h^2\right)(12F+6h)\frac{h^4}{24}\right)$$

$$c_{15}=\frac{h_\theta}{24h}-Nr\frac{h_\Omega}{24h}\left(1+\frac{Nt}{Nb}\right)-Rb\frac{h_\chi}{24h}(1-Pe\sigma)h^4+\left(\frac{Pr\,N\,b}{120h^2}+\frac{Pr\,N\,t}{120h^2}+\frac{RbPe}{120h^2}\right)h^5$$

References

[1] Latham T.W (1966) Fluid motion in a peristaltic pump. MS. Thesis. M.I.T. Cambridge.

[2] Jaffrin M. Y, Shapiro A. H (1971) Peristaltic Pumping. Annu. Rev. Fluid Mech. 3: 13-16. https://doi.org/10.1146/annurev.fl.03.010171.000305

[3] Hayat T, Anum Tanveer, Humaira Yasmin, Alsaedi A (2014) Effects of convective conditions and chemical reaction on peristaltic flow of Eyring-Powell fluid. Appl Bionics Biomech. 11(4): 221-233. http://dx.doi.org/10.3233/ABB-140100

[4] Ambreen A Khan, Fouzia Masood, Ellahi and Bhatti M.M (2018) Mass transport on chemicalized fourth-grade propagating peristaltically through a curved channel with magnetic effects. J. Mol. Liq. 258: 186-195.10.1016/j.molliq.2018.02.115

[5] Nooren Sher Akbar (2014) Peristaltic sisko nanofluid in an asymmetric channel. Appl Nanosci. 4(6): 663-673.

[6] Nooren Sher Akbar, Raza M and Ellahi (2016) Impulsion of Induced magnetic field for Brownian motion of nanoparticles in peristalsis. Appl Nanosci. 6: 359-370.
[7] Bhatti M. M, Zeenshan A and Ellahi R (2017) Electro magnetohydrodynamic (EMHD) Peristaltic flow of solid particles in a third grade fluid with heat transfer. Mech. Ind. 18(3): 314-323.DOI: 10.1051/meca/2016061
[8] Mekheimer K.H.S (2005) Peristaltic transport of Newtonian fluid through uniform and non-uniform annulus. Arab. J. Sci. Eng. 30: 69-83.
[9] Noreen Sher Akbar, Nadeem S, Hayat T, Awatif A. Hendi (2012) Erratum to: Peristaltic flow of a nanofluid in a non-uniform tube. Heat Mass Transfer. 48(3):451–459. DOI 10.1007/s00231-011-0892-7
[10] Ellahi R, Mubashir Bhatti M, Vafai K (2014) Effects of heat and mass transfer on peristaltic flow in a non-uniform rectangular duct. Int. J. Heat Mass Transf. 71: 706–719. http://dx.DOI: 10.1016/j.ijheatmasstransfer.2013.12.038
[11] Asha S. K and Sunitha G (2018) Mixed Convection Peristaltic Flow of a Eyring-Powell Nanofluid with Magnetic Field in a Non-Uniform Channel. Journal of Applied Mathematics and Computation. 2(8): 332-344.http://dx.doi.org/10.26855/jamc.2018.08.003
[12] Asha S. K, Sunita G (2017) Effect of Couple Stress in Peristaltic Transport of Blood Flow by Homotopy Analysis Method. AJST. 8(12): 6958-6964.
[13] Choi SUS (1995) Enhancing thermal conductivity of fluids with nanoparticle, In Developments and applications of non-Newtonian Flows. ASME. 99: 12-17.
[14] Choi SUS (2009) Nanofluids: From vision to reality through research. J Heat Transf Trans. 131(3): 033106. doi:10.1115/1.3056479
[15] Powell RE, Eyring H (1994) Mechanism for the relaxation theory of viscosity. Nature. 154(55): 427-428.
[16] Abbasi F.M, Alsaedi A, Hayat T (2014). Peristaltic Transport of Eyring-Powell fluid in a curved channel. J. Aerosp. Eng. 04014037-1-04014037-1.
[17] Asha S. K and Sunitha G (2018) Effect of joule heating and MHD on peristaltic blood flow of Eyring-Powell nanofluid in a non-uniform channel. JTUSCI. 13(1): 155-168. https://doi.org/10.1080/16583655.2018.1549530
[18] Noreen S, Qasim M (2013) Peristaltic flow of MHD Eyring-Powell fluid in a channel. Eur. Phys. J. Plus. 128(91): 1-10. DOI 10.1140/epjp/i2013-13091-3
[19] Hayat T, Irfan Shah S, Ahmad B and Mustafa M (2014) Effect of slip on peristaltic flow of Powell-Eyring fluid in a symmetric channel. Appl Bionics Biomech. 11: 69-79. DOI: 10.1155/2014/867328
[20] Abbasi F.M, Hayat T and Alsaedi A (2016) Numerical analysis for peristaltic motion of MHD Eyring-Prandtl fluid in an inclined symmetric cannel with inclined Magnetic field. J Appl Fluid Mech. 9(1): 389-396.
[21] Hina S, Mustafa M, Hayat T and Alsaedi A (2016) Peristaltic flow of Powell-Eyring in curved channel with heat transfer: A useful application in biomedicine. Comput Methods Programs Biomed. 135: 89-100. doi: 10.1016/j.cmpb.2016.07.019.
[22] Hayat Ali, Ahmed Abdulhadi (2017) Influence of magnetic field on peristaltic transport for Eyring-Powell Fluid in a Symmetric Channel during a porous medium. Math Theor Model. 9: 9-22.
[23] John R Platt (1961) Bioconvection patterns in cultures of free swimming organisms. Science. 133 (3466): 1766-1771. DOI:10.1126/science.133.3466.1766
[24] Pedley T. J, Hill N. A and Kessler J. O (1988) The growth of biconvection patterns in a uniform suspension of gyrotactic microorganisms. J. Fluid Mech. 195: 223-237. doi:10.1017/ S0022112088002393
[25] Avramenko A. A and Kuznetsov A. V (2004) Stability of a suspensions of gyrotactic micoorgansims in superimposed fluid and porous layers. Int. Commun. Heat mass transfer. 31(8): 1057-1066. http://dx.doi.org/10.1016/j.icheatmasstransfer.2004.08.003
[26] Kuznetsov AV (2006) The onset of thermo-bioconvection in a shallow fluid saturated porous layer heated from below in a suspension of oxytactic microorganisms. Eur J Mech B. 25: 223-233. https://doi.org/10.1016/j.euromechflu.2005.06.003
[27] Sampath Kumar P. B, Gireesh B. J, Mahanthesh B and Ali J Chamkha (2018) Thermal analysis of nanofluid flow containing gyrotactic microorgansims in bioconvection and second order slip with convective conditions. J Therm Anal Calorim. https://doi.org/10.1007/s10973-018-7860-0
[28] Kuznetsov and Avramenko (2004) Effect of small particle on the stability of bioconvection in a suspension of gyrotatic micro-organism in a layer of finite depth. Int Commun Heat mass. 31(1): 1-10. DOI: 10.1016/S0735-1933(03)00196-9
[29] Kuznetsov Andrey V (2011) Nanofluid bioconvection in water-based suspensions containing nanoparticles and oxytactic microorganism: oscillatory instability. Nanoscale Res. Lett. 100(6): 1-13. https://doi.org/10.1186/1556-276X-6-100

[30] Kalidas Das, Pinaki Ranjan Duari and Prabir Kumar Kundu (2015) Nanofluid bioconvection in presence of gyrotactic microorganisms and chemical reaction in a porous medium. JMST. 29 (11): 4841-4849. DOI 10.1007/s12206-015-0131-z

[31] Mehryan S.A.M, Farshad Moradi Kashkooli, Soltani M and Kaamran Raahemifar (2016) Fluid Flow and Heat Transfer Analysis of a Nanofluid Containing Motile Gyrotactic Micro-Organisms Passing a Nonlinear Stretching Vertical Sheet in the Presence of a Non-Uniform Magnetic Field; Numerical Approach. PLOS ONE. 11(6): 1-32. https://doi.org/10.1371/journal.pone.0157598

[32] Rakeshkumar, Shilpa Sood, Sabir Ali Shehzad and Mohsen Sheikholeslami (2017) numerical modeling of time-dependent bio-convection stagnation flow of nanofluid in slip regime. Results in Physics. 7: 3325-3332. https://doi.org/10.1016/j.rinp.2017.08.059

[33] Anwar Beg O, Prasad V R and Vasu B (2013) numerical study of mixed bioconvection in porous media saturated with nanofluid containing oxytactic microorganisms. J. Mech. Med. Biol. 13(4): 1-25. DOI: 10.1142/S021951941350067X

[34] Mutuku W. N, Makinde O. D (2004) Hydromagnetic bioconvection of nanofluid over a permeable vertical plate due to gyrotactic microorganisms. Comput. Fluids. 95: 88 – 97. DOI: 10.1016/j. compfluid.2014.02.026

[35] Saini S and Sharma Y. D (2018) A Bio-Thermal Convection in Water-Based Nanofluid Containing Gyrotactic Microorganisms: Effect of Vertical Through flow. JAMFM. 11(4): 895-903. DOI:10.29252/jafm.11.04.28062

[36] Aurang Zaib, Mohammad Mehdi Rashidi and Ali j Chamkha (2018) Flow of anofluid containing gyrotactic microorganism over static wedge in darcy-brinkman porous medium with convective boundary condition. Journal of porous media. 21 (10): 911-928. **DOI:** 10.1615/JPorMedia.2018019967

[37] Noor Saeed khan (2018) Biconvection in second grade nanofluid flow containing nanoparticles and gyrotactic microorganisms. Beazilian Journal of physics. 48(3): 227-241. https://doi.org/10.1007/s13538-018-0567-7

[38] Nooren Sher Akbar (2015) biconvection peristaltic flow in an asymmetric channel filled by nanofluid containing gyrotactic microorganism: Bio nano engineering model. Int J Numer Method H. 25(2): 214-224. http://dx.doi.org/10.1108/HFF-07-2013-0242

[39] Bhatti M. M, Zeeshan A and Ellahi R (2017) simultaneous effects of coagulation and variable magnetic field on peristaltically induced motion of Jeffrey nanofluid containing gyrotactic microorganism. Microvas Res. 112: 32-42. https://doi.org/10.1016/j.mvr.2016.11.007

[40] Gupta V. G and Sumit Gupta (2012) Application of homotopy analysis method for solving nonlinear Cauchy Problem. Surveys in mathematical and its applications. 7: 105-116.

[41] Hussain Q, Latif T, Alvi N and Asghar S (2018) Nonlinear radiative peristaltic flow of hydromagnetic fluid through porous medium. Results in Physics. 9: 121-134. https://doi.org/10.1016/j.rinp.2018.02.014